Applied Scientific Research **55:** 311–326, 1996.

Turbulent Drag Reduction by Spanwise Wall Oscillations

ARTURO BARON and MAURIZIO QUADRIO
Dipartimento di Ingegneria Aerospaziale, Politecnico di Milano, 40 via C. Golgi, 20133 Milano, Italy

Received 7 July 1995; accepted in revised form 10 April 1996

Abstract. In the present work a technique is numerically investigated, which is aimed at reducing the friction drag in turbulent boundary layers and channel flows. A cyclic spanwise oscillation of the wall with a proper frequency and amplitude is imposed, allowing a reduction of the turbulent drag of up to 40%. The present work is based on the numerical simulation of the Navier–Stokes equations in the simple geometry of a plane channel flow. The frequency of the oscillations is kept fixed at the most efficient value determined in previous studies, while the choice of the best value for the amplitude of the oscillations is evaluated not only in terms of friction reduction, but also by taking into consideration the overall energy balance and the power spent for the motion of the wall. The analysis of turbulence statistics allows to shed some light on the way oscillations interact with wall turbulence, as illustrated by visual inspection of some instantaneous flow fields. Finally, a simple explanation is proposed for this interaction, which leads to a rough estimate of the most efficient value for the frequency of the oscillations.

Key words: turbulence, turbulent drag reduction

1. Introduction

To date both numerical and experimental evidence exist [1, 2] that a sudden spanwise pressure gradient applied to a fully developed, two-dimensional turbulent boundary layer or channel flow can temporarily alter the structure of turbulence, leading to a transient decrease of turbulent quantities such as turbulence kinetic energy and turbulence production. If the spanwise pressure gradient is sustained in time, however, after the transient stage the flow adjusts to the new two-dimensional state, becoming aligned with the resultant, higher velocity, and the turbulence quantities return to their natural behaviour.

A spanwise cross-flow which oscillates in time has been shown by Jung et al. [3] and by Laadhari et al. [4], to be an effective mean for achieving *sustained* modifications of wall turbulence, ultimately leading to a significant turbulent drag reduction. When the imposed cross-flow oscillates with a period $T_{\mathrm{osc}}^{+} = 100$ and a flow-rate per unit width of $0.8Q_x/2h \sin(\omega t)$, Q_x being the streamwise flow rate for the unperturbed flow and h the channel half-height, Jung et al. have shown that up to 40% of sustained reduction of turbulent friction drag is possible. This constitutes an active drag reduction technique, since some auxiliary power is required, but no

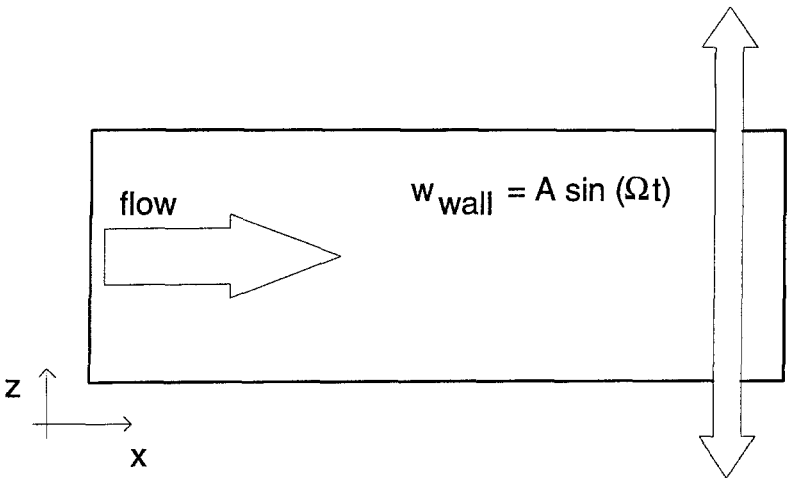

Figure 1. Schematic of wall oscillations.

feedback law or control algorithms are needed, so that practical realization of such a device may not be exceedingly complex.

The spanwise oscillatory motion of the walls (Figure 1) is perhaps more interesting from a practical point of view: although it works in a different way, this method has been shown by Jung to have an equivalent overall effect in terms of drag reduction and influence on the main turbulence statistics.

The basic mechanism by which spanwise oscillations can alter the turbulence structure near the wall is explained by Laadhari as the modification of the interaction between the fluid-pumping longitudinal vortices and the streaky pattern of the flow near the wall, which results to be displaced by the spanwise flow relative to the vortices. The central role of longitudinal vortices and, in general, of near-wall flow structures in the overall process of turbulence production and regeneration has been clearly underlined, among others, by Robinson [5].

Frequency and amplitude of the oscillations obviously play a first-order role in determining the amount of turbulent drag reduction. The performances of the oscillating wall (and of the oscillatory cross-flow) have been established by Jung through a parametric study, performed by numerical simulations, in terms of percentage of friction reduction. The choice of the optimum parameters, however, still has to be defined, by taking into account not only the savings in longitudinal friction, but rather the global energetic balance, which must guarantee that the amount of saved friction power is larger than the power spent to sustain the oscillation of the wall. In addition, turbulence statistics have not been fully documented yet, and an accurate examination of instantaneous flow fields is still missing.

In this paper, with the aid of numerical simulations of a plane turbulent channel flow, we consider the energetic aspect of this drag reduction technique, focusing our attention on the key parameter represented by the amplitude of the oscillations

of the wall. Turbulence statistics are presented, with the aim of understanding the mechanism by which spanwise oscillations can reduce drag.

2. The numerical method

The computer code developed and used for the simulations presented in the following is a standard solver for the Navier–Stokes equations, in the simple geometry of a plane channel flow. It is based on second order finite differences schemes, and takes advantage of a partially implicit algorithm (Crank–Nicholson for the viscous terms and third-order Runge–Kutta for the convective terms) for advancing in time the solution. The standard periodic boundary conditions in the streamwise (x) and spanwise (z) directions are used, and the no-slip condition is imposed at the channel walls. The movement of the walls is directly considered via the boundary condition for the spanwise component of the velocity. Spanwise cross-flow simulations are not considered in the present work.

The computations are performed with a fixed longitudinal flow rate Q_x, with a Reynolds number (based on the friction velocity u_τ and on the half-height h of the channel) of $\mathrm{Re}_\tau = 200$. A lower Re_τ could have several advantages, but we decided to use the value 200 both to enable a direct comparison with the results of Jung et al., and to allow a fully turbulent flow even in those simulations where the amount of drag reduction is significant.

The grid used for the discretization of the computational domain is $54 \times 120 \times 60$ in the streamwise, normal to the wall and spanwise directions respectively, allowing a spatial resolution which is sufficient to resolve all the essential scales of the turbulent motion. The dimensions of the domain in the streamwise and spanwise directions are of $4.05h$ and $2.5h$, respectively. These dimensions are certainly not sufficient to support the claim that we have performed a *Full Channel* simulation (as in [6]). In this case the dimensions have to be set a priori, following, for example, the suggestion of Kim and Moin [7], and then checked a posteriori. On the other hand, the present dimensions largely exceed those implied by the *Narrow Channel* assumption. According to this idea, presented first by Jiménez and Moin [8], the computational domain has to be wide and long enough for the dynamically most important flow structures to accommodate. When scaled in wall units, these minimal dimensions are approximately independent of the Reynolds number, and are around 100 wall units in span and 250–350 wall units in stream. While much cheaper than its counterpart, a *Narrow Channel* simulation can provide a great amount of information, and Jiménez has shown that the near-wall flow is well represented by such a simulation, while the outer flow is certainly affected by the limited size of the computational domain.

All the computational cases are started from the same, unmanipulated flow field. They are advanced in time for 800 viscous time units, allowing the flow to stabilize, and then integrated further 800 viscous time units in order to compute the turbulence statistics. A HP Series 700 workstation is used, with a central memory

of 64MB. The size of the computational domain has been chosen in order to obtain an "in core" simulation. The single time step takes approximately 30 CPU seconds, for a total time of approximately 40 CPU hours for each of the cases illustrated in the following. Further details regarding the adopted algorithms and the numerical schemes can be found in Baron and Quadrio [9].

3. Energy Budget

Several computations have been performed, in order to assess the turbulent drag reduction properties of the oscillating wall for practical applications. For this purpose, we have considered not only the potential benefit in terms of longitudinal skin friction reduction, but we have also taken into account the penalty associated with the power spent to sustain the oscillation of the wall. The power saved is simply defined as $(-\mathrm{d}p/\mathrm{d}x|_u + \mathrm{d}p/\mathrm{d}x|_o)U_{\mathrm{bulk}}$, where the suffices indicate the unmanipulated and the oscillating case, and U_{bulk} is the bulk mean velocity. The power spent is defined as $\int \tau_{wz} \cdot w_{\mathrm{wall}}\, \mathrm{d}S$: this surface integral has been hence computed and integrated in time. For this parametric study, the period of the oscillation has been set to the value of $T^+_{\mathrm{osc}} = 100$, which should allow the best performances in terms of drag reduction, according to the work of Jung et al. It is clear that a full study of this two-parameter problem, varying both the amplitude and the period of the oscillations, is needed in order to draw definitive conclusions on the quantitative performances of the oscillating wall. Nevertheless, this choice for the period allows meaningful estimations without the expense of a computationally intensive full parametric study. The amplitude of the velocity oscillations, which take place in a sinusoidal way, varies from zero (fixed wall) up to $1.0Q_x/2h$ with a step of 0.25. The imposed spanwise velocity assumes quite high values: $1.0Q_x/2h$ corresponds to w^+ greater than 15. We keep in the present work the non-dimensionalization of the amplitude in terms of outer variables in order to compare with the results of Jung.

The results are summarized in Figure 2, where they are normalized by the longitudinal friction power for the unmanipulated case.

Considering first the performances of the oscillating wall in terms of friction drag reduction, the results of the present tests confirm the findings of Jung, indicating a maximum drag reduction of the order of 40% for values of the amplitude larger than $0.75Q_x/2h$. This amount of reduction is certainly appealing, compared with the best achievements of most passive drag reduction techniques (such as riblets) which can hardly reach 10%. A decrease in the amplitude leads to decreased benefits, which appear to diminish in a not exactly linear way. For an amplitude of $0.25Q_x/2h$ the overall balance appears to be positive, indicating a net benefit.

In conclusion, results from Figure 2 seem to indicate that potential savings in longitudinal friction are significant, but that a careful optimization of the oscillations is necessary in order to achieve a net gain, even in the ideal situation considered above.

Figure 2. Powers as a function of the amplitude of the wall velocity oscillation $Q_x/2h$, normalized with the friction power of the unperturbed case: friction power saved (white); power spent to the wall (grey); power budget (black).

4. Turbulence Statistics

Turbulence statistics have been computed for the case of the wall oscillating sinusoidally with an amplitude of $0.75Q_x/2h$ and with a period of $T^+_{\rm osc} = 100$. This case is very similar to the one documented by Jung ($0.80Q_x/2h$), and allows the achievement of the maximum drag reduction. The selected amplitude corresponds to a value of the spanwise wall velocity of $w^+ \cong 13$ or $w^+ \cong 16$, according to the choice of the (unperturbed or reduced, respectively) friction velocity. After the initial, transient stage, the statistics are computed for 20 cycles of oscillation.

The mean velocity profile has been reported both by Jung and by Laadhari. Both authors plot the profile using the friction velocity of the unmanipulated case. Jung does not find evidence of a law-of-the-wall behavior, and shows a profile which is less full near the wall when compared with the canonical one. Laadhari, on the other hand, reports a profile which resembles the standard shape but does not exactly coincide with the standard curve, which might be due to experimental differences in determining the friction velocity. In Figure 3 the mean velocity profile from the present computations is plotted, using both the friction velocities of the unperturbed case (dotted line) and of the manipulated case (dotted line with symbols). Jung's results are confirmed, and there is clear indication that, when the profile is plotted using its own friction velocity in the law-of-the-wall form, it does exhibit the usual upward shift in the logarithmic region, characteristic of other drag reducing flows [10].

The distribution in the direction normal to the wall of the root mean squared values for the fluctuations of the three velocity components are reported both by Jung and Laadhari. Both show significant reductions in the oscillating case.

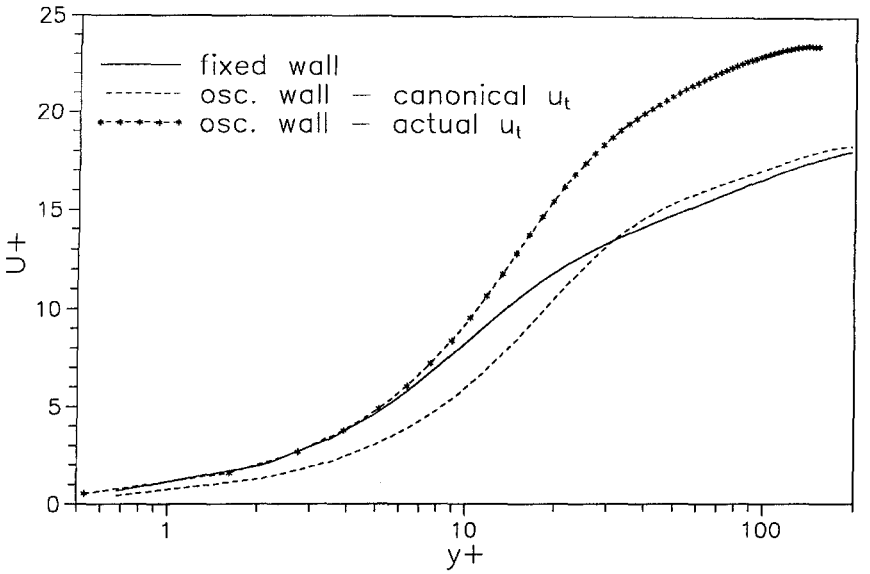

Figure 3. Mean velocity profile in the law-of-the-wall form.

Data from the present computation are shown in Figures 4a, b, c, for the three components of the velocity vector.

Except for an outward shift in the position of the peak, the streamwise component appears to be substantially unchanged when plotted with the actual u_τ, while its peak value is reduced when made non-dimensional with the u_τ of the unperturbed simulation. The outward shift in the position of the peak is recognizable also when examining the other two components. The fluctuations of both the components of velocity, for fixed and oscillating spanwise and normal-to-the-wall components are reduced throughout the whole channel, regardless of the friction velocity being used.

Root mean squared values for other turbulent quantities are computed. Reynolds shear stress (not reported here) have been found to fully confirm the findings of Jung et al., showing the expected reduction. It is interesting to observe the distribution, in the direction normal to the wall, of the RMS values of the fluctuations of vorticity (Figures 5a, b, c). The streamwise component (Figure 5a) shows a general behavior similar to the reference case with fixed wall, but the distribution assumes lower values in the oscillating case. In particular, the wall value of the streamwise vorticity RMS fluctuations is approximately halved. Even the normal component (Figure 5b) appears to be reduced throughout the whole channel, with the shape of its profile approximately unchanged. When the actual u_τ is used, the outward shift in the position of its maximum is obviously reduced. The spanwise component (Figure 5c) appears to be significantly altered by the oscillations, showing a local

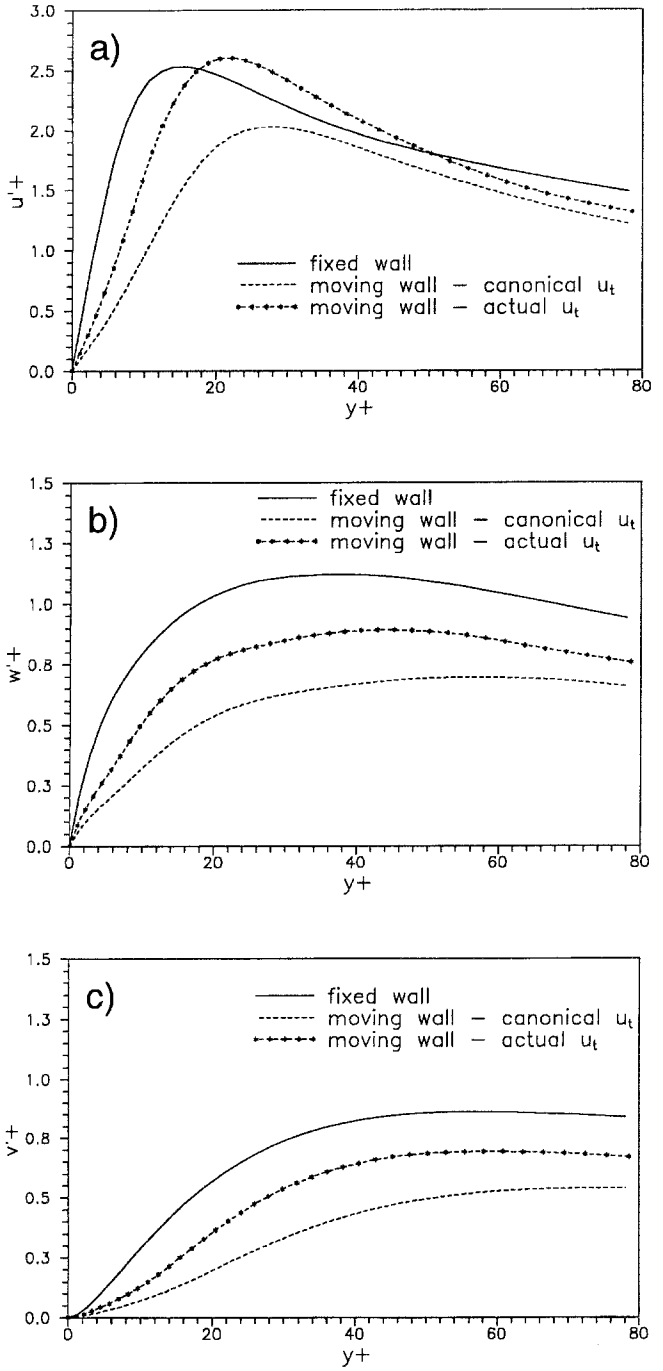

Figure 4. Profiles of rms values for the three components of velocity, for fixed and oscillating walls: (a) streamwise; (b) spanwise; (c) normal.

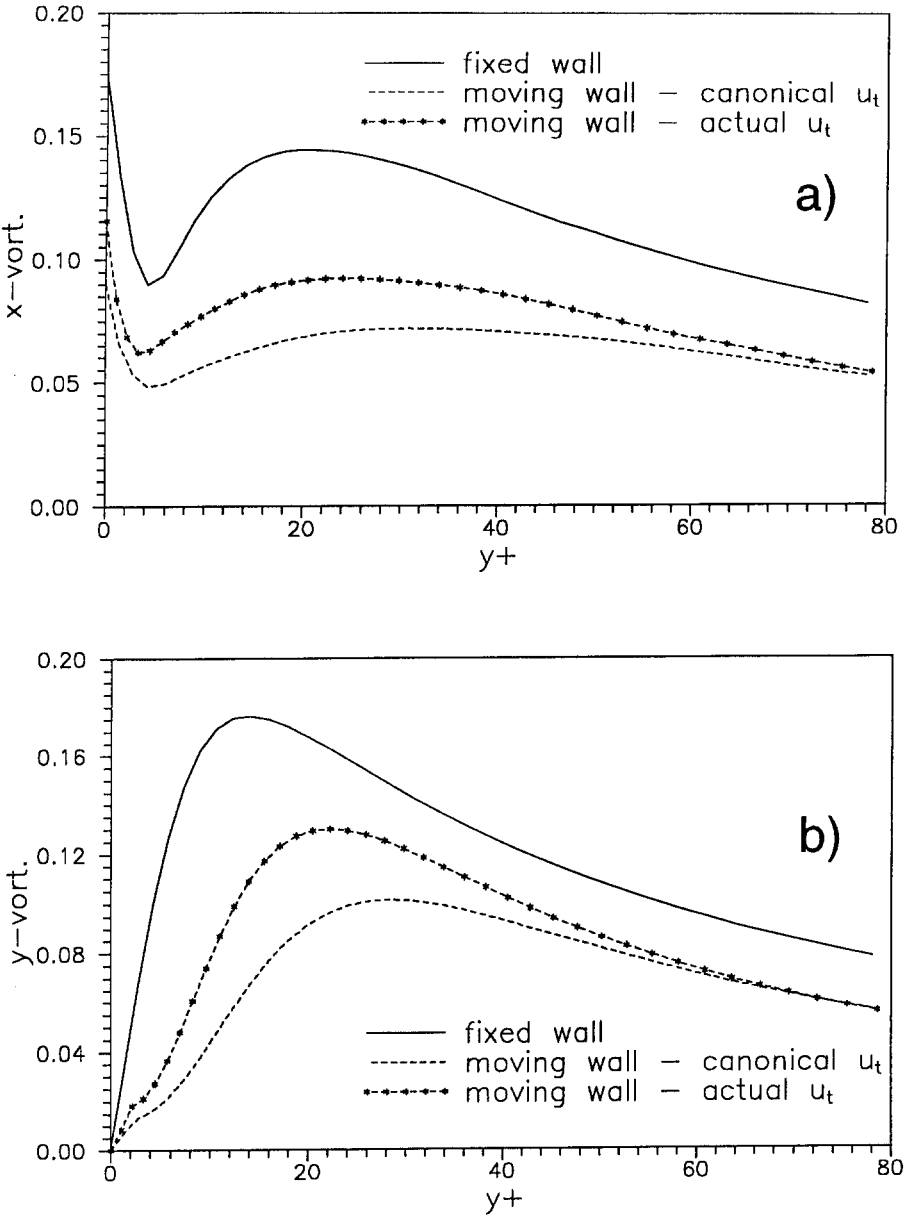

Figure 5. Profiles of rms values for the three components of vorticity and pressure fluctuations: (a) streamwise vorticity; (b) normal vorticity; (c) spanwise vorticity; (d) pressure.

maximum around 15 wall units from the wall, a local minimum at $y^+ \cong 5$ and a decreased wall value.

Figure 5d shows the root mean squared values for the fluctuations of pressure. A significant modification induced by the oscillations of the wall can be observed.

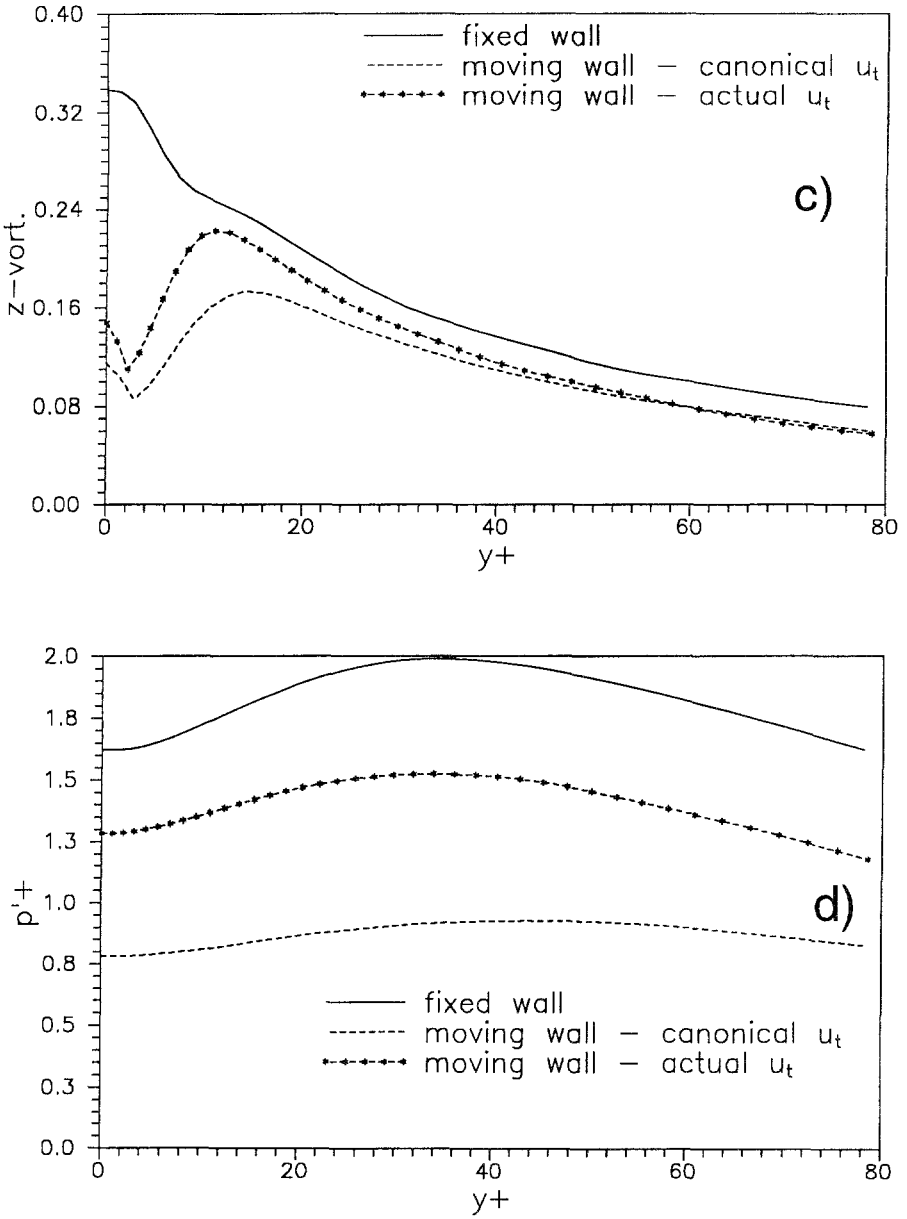

Figure 5. (Continued)

The amount of this change is, as usual, highly dependent on the choice of the friction velocity used in plotting the data, but anyway a reduction of the pressure fluctuations seems to be unquestionable, especially for the peak value near the wall.

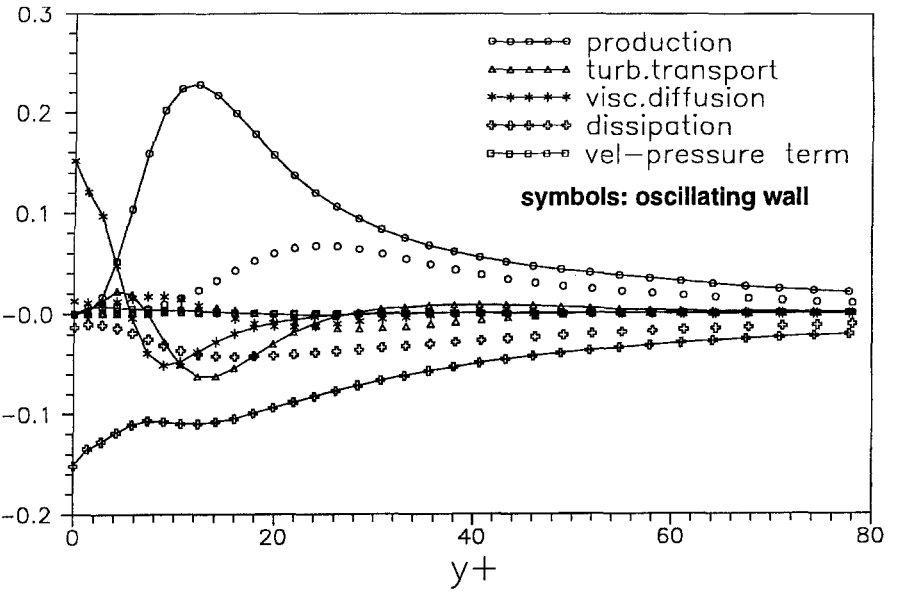

Figure 6. Terms in the budget of the turbulence kinetic energy. Line with symbols: fixed wall. Symbols: oscillating wall.

In Figure 6 are reported the distributions, in the direction normal to the wall, of the various terms which contribute to the budget of the trace of the Reynolds stress tensor, i.e. the turbulence kinetic energy K. For an exact definition of all these terms, the reader is referred, for example, to the work by Mansour et al. [11].

The figure only shows the curves computed with the unmanipulated friction velocity. The continuous lines with symbols represent the canonical case, and the symbols stand for the oscillating wall. In some profiles (like production of K) a shift towards the interior of the channel can be observed. The more evident effect is however the reduction of all the terms in the near-wall region, particularly noticeable for those terms that assume high wall values in the reference case. The dissipation $-\varepsilon_{ij} = -2\nu\partial u_i/\partial x_k \partial u_j/\partial x_k$, for example, shows a reduction of an order of magnitude in the value at the wall. Similar behavior can be noted for the profile of the viscous diffusion $\nu\partial^2\overline{u_i u_j}/\partial x_k$. Both the mentioned profiles also reveal a general shape which is quite different from the canonical case, loosing the characteristic of maximum at the wall.

Some major changes are discernible in the near-wall region in the distributions of the skewness and flatness factors for the fluctuations of the three velocity components (Figure 7). The third moment (skewness) for the streamwise component, for example, exhibits higher values in the wall region, with a local maximum which is no more at the wall, but at approximately 5–10 wall units far. As in the unperturbed case, the skewness factor of the fluctuations for the spanwise component of the velocity approximately assumes the value of zero, due to the reflection properties

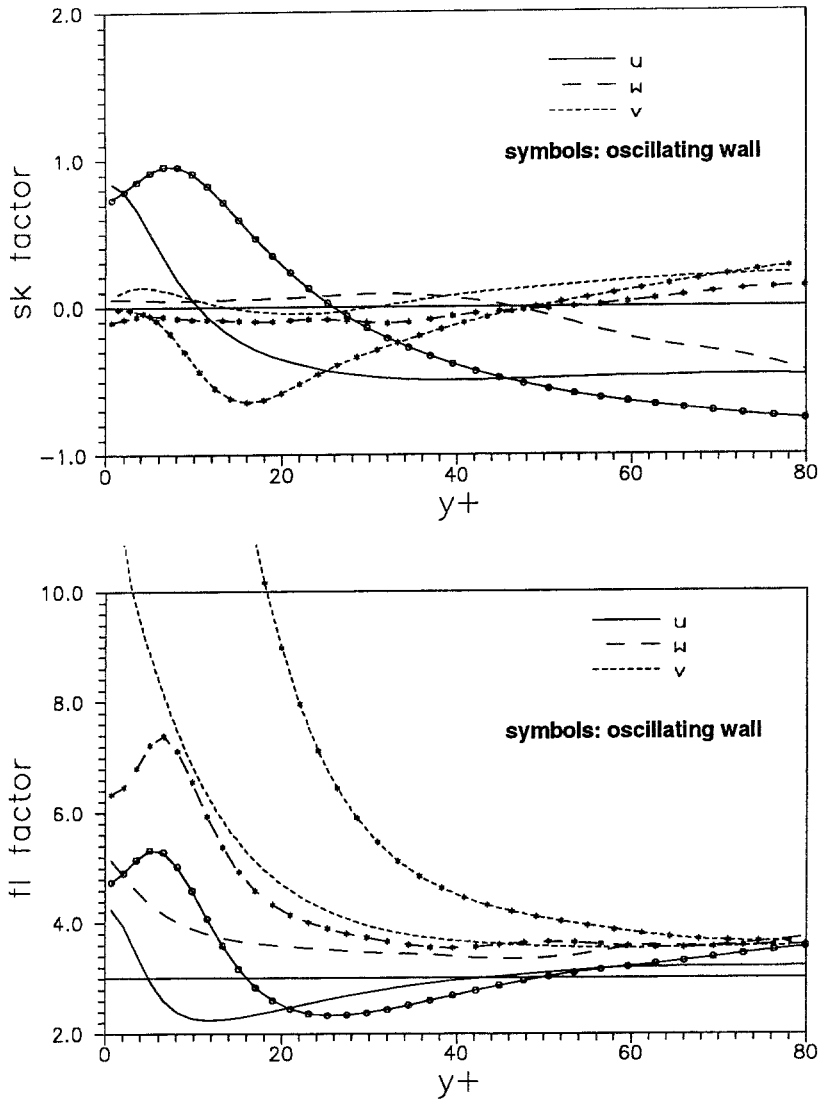

Figure 7. Skewness and flatness factors for the three velocity components.

of the Navier–Stokes equations. The normal velocity component presents a region of negative skewness for $5 < y^+ < 40$, with a negative peak around $y^+ \approx 15$. Regarding the flatness factors, the streamwise component presents a local maximum and a slightly higher wall value, and the spanwise component shows a similar behavior. The profile for the normal component assumes values at the wall, which are very high and superior to those of the fixed wall case.

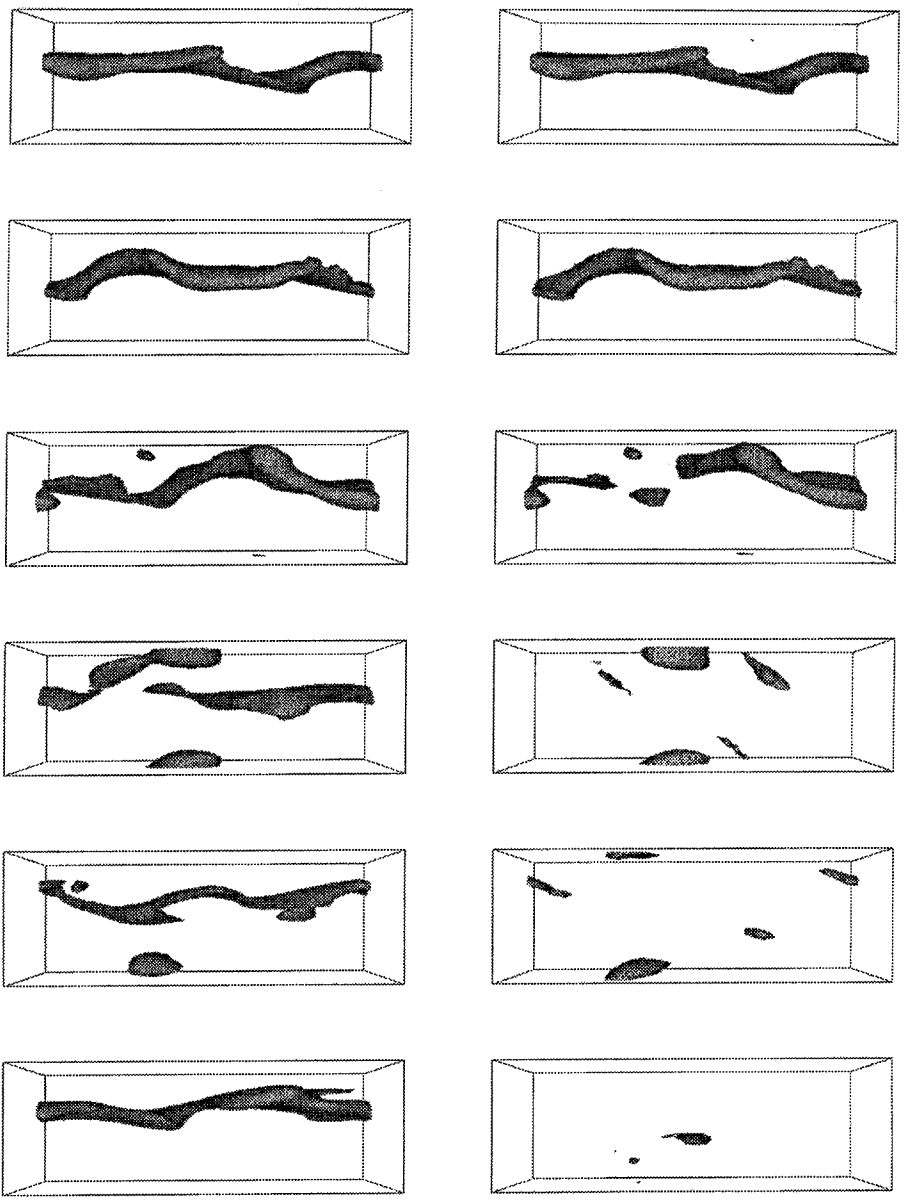

Figure 8. Isosurfaces for fluctuations of streamwise velocity $u^+ = -3.0$, for the fixed (left) and the oscillating (right) cases. Perspective, top view of the lower half of the channel, taken from the centerplane. Flow is from left to right, at $\mathrm{Re}_\tau = 140$. Time is from top to bottom: $t^+ = 0, 12.5, 25, 50, 75, 100$. In each case the actual, instantaneous friction velocity is used.

5. Instantaneous Flow Fields

The direct, visual inspection of turbulent flow fields can be a very useful tool for understanding the complex turbulence near-wall dynamics. In addition, the *Narrow Channel* technique [8] allows to isolate a small number of significant structures and to easily follow their evolution in time. Visualisation of data produced with the *Narrow Channel* technique is illustrated on Figures 8 and 9. The computations have been performed on a $32 \times 90 \times 32$ grid, covering a computational domain which is $3.0h$ long and $1.0h$ wide. The Reynolds number has been set to the relatively low value of $\mathrm{Re}_\tau = 140$, in order to obtain larger and more detailed views. The evolution of the flow is followed for a time interval which corresponds to the entire first period of the oscillation, which takes place with the usual values of $T^+_{\mathrm{osc}} = 100$ and amplitude $0.75Q_x/2h$. In both figures the left column refers to the unmanipulated flow, and the right one to the corresponding flow in the oscillating case. The figures show a perspective top view of the lower half of the channel, taken from the centerplane; flow is from left to right; time is from top to bottom. The frames are for values of t^+ of 0, 12.5, 25, 50, 75 and 100.

An important point which is worth mentioning is the choice of the friction velocity for the setting of the threshold values. The structures are visualized by choosing a threshold value for the scalar quantity to be traced in time. This value is kept fixed when expressed in wall units, and since the friction velocity experiences a significant reduction in time during the examined time interval, the use of the value of u_τ from the canonical computations would have led to an obvious successive weakening of the structures as t^+ increases. By referring to the instantaneous (space-averaged) friction velocity, indeed, it is possible to have a better idea of the evolution in time of the structure itself.

Examining first the isosurfaces of the streamwise velocity component for the value $u^+ = -3$, in the unmanipulated case (Figure 8, left) a single low-speed streak is evident, which presents the typical meandering, and a subsequent loss of coherence followed by a regeneration process. In the oscillating case (Figure 8, right), the effect of the movement of the wall becomes apparent after one quarter of a period, as a drastical weakening of the streaky structure. At the end of the first cycle of oscillation, any trace of the original pattern is lost.

Figure 9 focuses on the isosurfaces of the product uv at the value $(uv)^+ = -3$. The spotty behavior, described among others by Jiménez and Moin [8], is discernible in the canonical case, while in the manipulated case a gradual weakening of the structures can be noticed.

It is clear that further, careful visual analysis of the data is needed, in order to gain definitive conclusions on the way the oscillating wall interacts with the near-wall turbulence structures. The analysis of some elementary pictures, as those reported in Figures 8 and 9, allows nevertheless to get an immediate idea of the globality of the modifications induced on the near-wall turbulence by the spanwise oscillations of the channel wall.

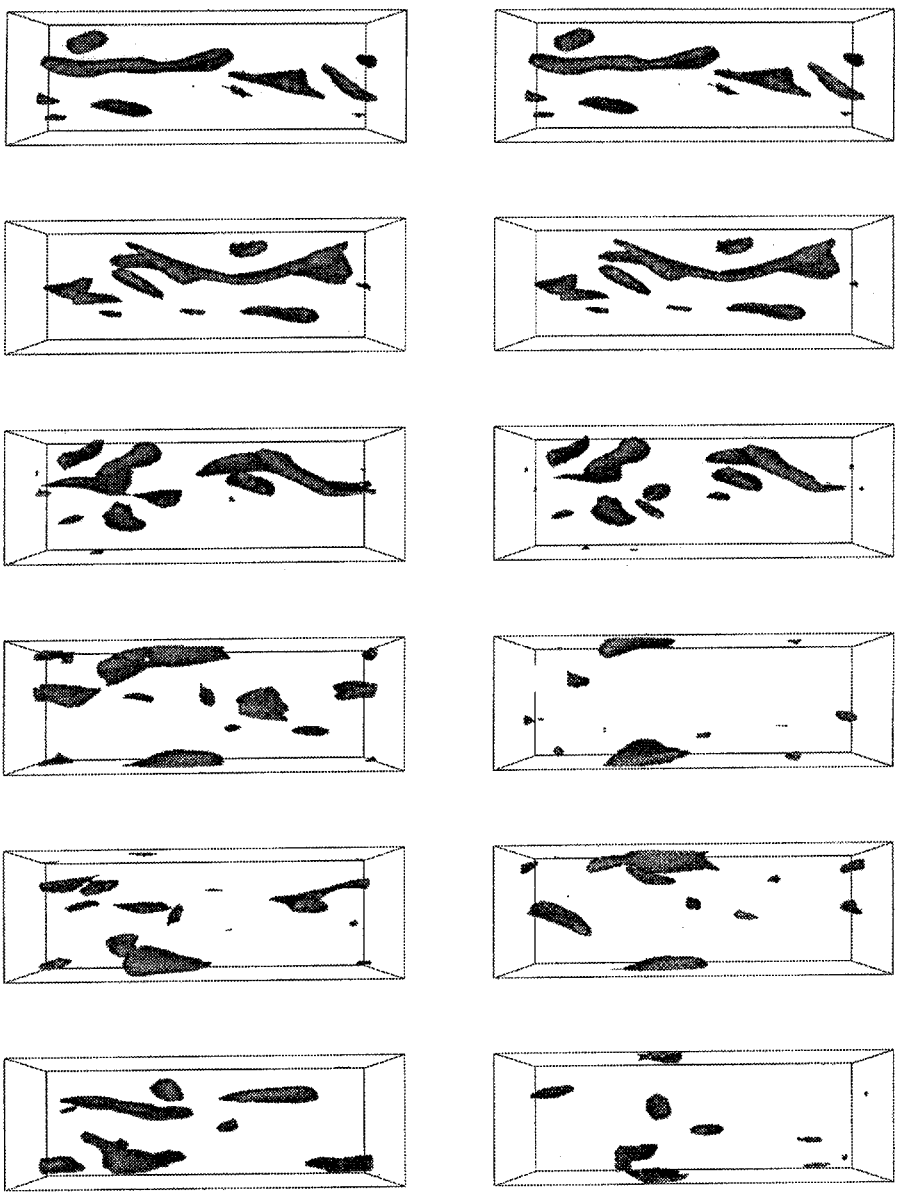

Figure 9. Isosurfaces for Reynolds stress $(uv)^+ = -3.0$, for the fixed (left) and the oscillating (right) cases. Perspective, top view of the lower half of the channel, taken from the centerplane. Flow is from left to right, at $\mathrm{Re}_\tau = 140$. Time is from top to bottom: $t^+ = 0$, 12.5, 25, 50, 75, 100. In each case the actual, instantaneous friction velocity is used.

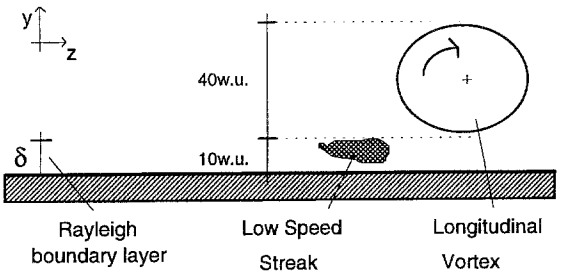

Figure 10. A conceptual model of the effect of spanwise oscillations.

6. A Simple Model

As it can be noted from the analysis of the turbulence statistics presented in the previous sections, the alteration of the structure of turbulence near the wall due to the oscillating motion of the wall is significant. A simple scheme for understanding the effect of such oscillations is to consider that spanwise motion of the wall (or, equivalently, spanwise alternate cross-flow) disrupts the spatial coherence between streamwise vortices and low velocity streaks. This very simple model allows a rough estimate of the optimum oscillation period, which turns out to be approximately $100\nu/u_\tau^2$ from the numerical, parametric, study by Jung et al. [3].

A high-frequency laminar oscillatory flow with frequency Ω above a flat plate (the so-called "Stokes second problem" in [12]) creates a boundary layer of thickness $\delta = y\sqrt{\Omega/2\nu} \cong 3$. In wall units, this amounts to $\delta^+ = \sqrt{4\pi T^+}$. The effect of the oscillations is felt up to the edge of this boundary layer. If the effectiveness of the oscillations in reducing turbulent drag is due to a relative displacement of low speed streaks and the above longitudinal vortices, the transverse boundary layer must embed as much of the streaks as possible without influencing the vortices, allowing the maximum relative displacement. Given that the streaks take place in the region $y^+ < 10$ and the streamwise vortices live on average in the region $10 < y^+ < 50$ (see Robinson, 1991), a value for the period of oscillation follows, which is approximately $T^+ \approx 100$.

7. Conclusions

Spanwise oscillation of the wall has been shown to be an effective method for achieving a sustained friction drag reduction for low Reynolds, wall bounded turbulent flows. The remarkable savings in friction are indeed counterbalanced by the power necessary to sustain the oscillation of the wall.

It has been shown that, in the case of the wall moving with a spanwise velocity which varies sinusoidally in time, a positive overall balance may be possible, if the amplitude of the velocity oscillation is kept low. This energetic balance is evaluated in an ideal situation, without accounting for losses due to mechanical

systems. Anyway, it is these authors' opinion that the technique can be further optimized, in order to reduce the energetic cost of its application.

Turbulence statistics have been reported, with the aim of highlighting the main modifications induced by the movement of the wall on the behavior of the wall turbulence. The major effect seems to be a reduction of the velocity fluctuations, mainly concerning the normal component. In addition, an outward shift of most profiles is apparent, with an amount approximately of the order of the thickness of the transverse boundary layer induced by the moving wall. Higher statistical moments of the velocity fluctuations show substantial variations in the shape of the profiles, and the examination of the terms contributing to the budget of the turbulent kinetic energy seems to support the idea that the transversal boundary layer produced by the oscillations is characterized by reduced turbulent activity.

Even if the use of spanwise oscillation of the wall as a technique for reducing turbulent drag will prove not to be feasible, its accurate comprehension will constitute a further tool for understanding and exploiting the relevance of local spanwise motions in the overall cycle of production and regeneration of turbulence.

Acknowledgments

This research has been partially supported by the Ministero dell'Università e della Ricerca Scientifica e Tecnologica during 1994.

Part of the contents of this paper was presented during the Euromech Colloquium 332, *Drag Reduction*, held at Ravello (Naples), April 1995.

References

1. Sendstad, O. and Moin, P., *On the Mechanics of 3-D Turbulent Boundary Layer.* Proceedings of the Eight Symp. on Turbulent Shear Flows, Munich, 1991.
2. Bradshaw, P. and Pontikos, N.S., Measurements in the turbulent boundary layer over an 'infinite' swept wing. *Journal of Fluid Mechanics* 159 (1985) 105–130.
3. Jung, W.J., Mangiavacchi, N. and Akhavan, R., Suppression of turbulence in wall-bounded flows by high-frequency spanwise oscillations. *Physics of Fluids A* 4(8) (1992) 1605–1607.
4. Laadhari, F., Skandaji, L. and Morel, R., Turbulence reduction in a boundary layer by a local spanwise oscillating surface. *Physics of Fluids A* 6(10) (1994) 3218–3220.
5. Robinson, S.K., Coherent motions in the turbulent boundary layer. *Annual Review of Fluid Mechanics* 23 (1991) 601–639.
6. Kim, J., Moin, P. and Moser, R., Turbulence statistics in fully developed channel flow at low Reynolds number. *Journal of Fluid Mechanics* 177 (1987) 133–166.
7. Kim, J. and Moin, P., Numerical investigation of turbulent channel flow. *Journal of Fluid Mechanics* 118 (1982) 341–377.
8. Jiménez, J. and Moin, P., The minimal flow unit in near-wall turbulence. *Journal of Fluid Mechanics* 225 (1991) 213–240.
9. Baron, A. and Quadrio, M., Direct numerical simulation of turbulent flows under the *Narrow Channel* assumption. *L'Aerotecnica Missili e Spazio* 73(1) (1994) 3–13.
10. Choi, K.-S., Near-wall structure of a turbulent boundary layer with riblets. *Journal of Fluid Mechanics* 208 (1989) 417–458.
11. Mansour, N.N., Kim, J. and Moin, P., Reynolds-stress and dissipation-rate budgets in a turbulent channel flow. *Journal of Fluid Mechanics* 194 (1988) 15–44.
12. Schlichting, H., *Boundary Layer Theory.* New York: McGraw-Hill (1968).